COMPARISON OF TWO METHODS TO CALCULATE EXTERNAL LOADS AT FLIGHT IN CONTINUOUS TURBULENCE

Bohdan HEVKO [ID]*, Yurij BONDAR [ID]

Department of Aircraft and Rocket Engineering, Igor Sikorsky Kyiv Polytechnic Institute, Kyiv, Ukraine

Abstract. The external loads from the continuous turbulence on the elastic high aspect ratio wing of the transport category aircraft are calculated by Dynamics of Turbulence Air (DTA) and Interactive Multidisciplinary Aircraft Design (IMAD) methods. The response to continuous turbulence was determined taking into account the requirements of CS-25.341(b). The model of the aircraft structure is directed by symmetrical spatial beam schematization. Determination of aerodynamic forces and moments was performed using the methods of linear computational aerodynamics: the panel method of Doublet-Lattice and Constant Pressures (DLM/CPM) and the method of circulation. Comparison of the results of load determination showed that, in general, the values of the loads calculated using IMAD are lower than the values calculated using DTA. Therefore, when designing an aircraft, it is advisable to combine these methods: calculate the loads using IMAD, as a more functional method, and then the loads obtained in the critical points of the calculated flight area should be confirmed using the DTA method. Thus, this study determined the difference between the results of the calculation of loads from the continuous turbulence on the elastic wing of the transport category aircraft using DTA and IMAD methods.

Keywords: continuous turbulence, aircraft wing, external loads, spatial-beam schematization, method of circulation, doublet-lattice method, constant pressures method.

Introduction

One of the areas of interest for studying in the aviation industry is the determination of dynamic loads acting on the aircraft structure. This is an extremely important problem for aviation. Improving the accuracy of the solution to this problem will be related to studies in various areas, such as aerodynamics, flight dynamics, and strength and control systems. Dynamic loads occur when flying in turbulent conditions, passing through a concomitant vortex track of another aircraft, etc. Thus, flight in turbulent conditions is one of the main design cases for determining the strength under the influence of dynamic loads, especially the strength of the wing, fuselage, and engine mount.

A significant amount of work is devoted to solving the problem of determining the loads and ensuring the strength of the aircraft structure during the flight in turbulent conditions. Thus, Kim and Hwang (2004) analyse the reliability of the composite wing which was exposed to gust loads using Monte Carlo method modelling to handle random variables and numerical results. As gust profile is continuous and irregular, a continuous gust profile is described as a stationary Gaussian stochastic process and

is widely used to analyse gust loads. The processing of random variables and numerical results showed that the failure probability increases nonlinearly as the Root-Mean-Square (RMS) gust rate increases. When using a high aspect ratio and flexible wings, the impact of gusts on the design of the aircraft becomes more significant. In another paper (Reytier et al., 2012) an effective numerical method is proposed for generating correlated stress time histories for airplane structures that are exposed to air loads. The authors also considered random air gusts acting in any direction and leading to random multi-axis loads on the structure of the aircraft. Another way to estimate the load of the aircraft during flights in turbulent conditions was proposed by Fomichev et al. (2014). Their method is based on the determination of integral repeatability of overload of an aircraft in flight.

Unexpected gusts can endanger flight safety. Consequently, Gust Load Alleviation (GLA) is a one of the key problems of aeroelasticity. In the paper "Model Predictive Control for Gust Load Alleviation" (Giesseler et al., 2012), the authors propose to reduce gust loads in critical areas of an aircraft construction using Light Detection

---

*Corresponding author. E-mail: *bahevko@gmail.com*

And Ranging (LIDAR) systems. Tang et al. (2016) in their paper investigated existing scaling laws of the GLA control system and formulated basic scaling criteria for the proportional–integral–derivative control system. Also, the authors have proposed and verified a scaling methodology which can directly relate gust response of the full-size aircraft to the scaled model.

The structure of modern aircraft demands the evaluation of dynamic loads caused by discrete and turbulence gusts. At certain loads from air gusts on the aircraft, as a rule, one-dimensional gusts are used (European Union Aviation Safety Agency [EASA], 2020). The field of these gusts has a uniform distribution by spanwise. Unfortunately, this profile cannot accurately reproduce a valid gust field. There are practically no methods for calculating dynamic reactions of a two-dimensional discrete gust. Such common software tools as NASTRAN (Rodden & Johnson, 1994) and ZAERO (ZONA Technology, 2017), are not suitable for detecting loads and reactions from non-uniform gusts (Karpel et al., 2005). Therefore, the study of two-dimensional discrete impulses has recently become popular (Yang et al., 2019; Lone & Dussart, 2019).

For fast-flowing processes such as the flight of an aircraft and the response of the elastic structure to external perturbations, it is important to determine the parameters of the processes and compare them with experimental results, which is impossible without the use of modern computer technologies. However, there is a problem of introducing new methods in engineering process. Usually, several basic software tools and methods are used, these are NASTRAN, ZAERO, DTA (Kuznetsov, 2008), and IMAD (Ivanteev et al., 2004). The principle of determining the loads on the aircraft when flying in turbulent conditions with the help of these methods is similar and in general corresponds the ones described by Wright and Cooper (2008) and by Kuznetsov (2008).

First of all, when designing an aircraft, it is necessary to determine the main components of the loads acting on the aircraft structure. For the wing, it is the distribution of shear force, torque and bending moment, and vertical overload over the wingspan. During the study, it is necessary to determine the loads on the aircraft structure and to compare the existing methods of determining the loads that occur when flying in turbulent conditions. Thus, the *purpose* of this work is to determine the difference between the results of the calculation of loads from the continuous turbulence on the elastic wing of the transport category aircraft using DTA and IMAD methods.

1. Methods to calculate the loads during the flight in turbulent conditions

In this study, DTA and IMAD methods which were worked out in Central Aerohydrodynamic Institute (romanized: Tsentral'nyy Aerogidrodinamicheskiy Institut, TsAGI), were used to determine the loads from continuous turbulence on the elastic wing of a transport aircraft. IMAD (Ivanteev et al., 2004) – is a method which is used
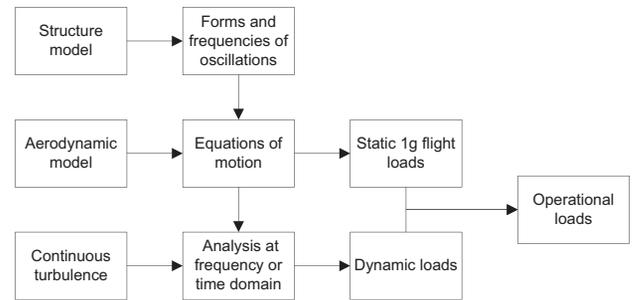
Figure 1. Block diagram for the calculation of external loads on an aircraft during flight in turbulent conditions (created by Authors)

to describe, develop and study a complete elastic mathematical model of an aircraft. The DTA method (Kuznetsov, 2008) is developed for calculation of dynamic loading of an elastic airplane with suspended objects when flying in turbulent conditions. The algorithm used in these methods to calculate the loads during the flight in turbulent conditions was studied before (Hevko & Bondar, 2019) and is presented in Figure 1.

According to Figure 1, the general order of the calculation of loadings on the plane during flight in turbulent conditions is defined. First, it is necessary to describe the elastic-mass model of the aircraft using: beam schematics, elastic discretely reinforced plates, Finite Element Model (FEM), and their combinations. The next step is to conduct a modal analysis of the structure where the frequencies and shapes of natural oscillations are determined by solving a common system of integral and linear equations using various methods: successive substitutions, Lanczos, or Simpson (Hevko & Bondar, 2019).

The third stage is to set the aerodynamic model of the surface of the aircraft using body, wing, or plane aerodynamics models and the flight mode (altitude, speed, etc.). The aerodynamic coefficients are then determined both for subsonic and supersonic flight speeds, with or without taking into account the unsteady aerodynamic characteristics using the following methods: defined circulations (Kuznetsov, 2008), DTA (Rodden et al., 1998, 1999), discrete stationary or non-stationary vortices, etc.

Knowing the forms of natural oscillations and having applied one or another aerodynamic theory, the equation of motion was obtained based on Lagrange equations of the second kind. Using the quasi-stationary approach the following matrix equation concerning the vector of generalized coordinates $\{q\}$ (Kuznetsov, 2008) was obtained:

$$\mathbf{C}\{\ddot{q}\}+\mathbf{D}\{\dot{q}\}+\mathbf{H}\{\dot{q}\}+\mathbf{B}\{q\}+\mathbf{K}\{q\}= \{R_U\}U(t)+\{R_\delta\}\delta(t), \tag{1}$$

where $\mathbf{C}$ – diagonal matrix of generalized masses; $\mathbf{D}$ – matrix of aerodynamic damping; $\mathbf{H}$ – matrix characterizing the structural damping; $\mathbf{B}$ – aerodynamic stiffness matrix; $\mathbf{K}$ – structure stiffness matrix; $\{R_U\}$ – vector representing the work of external forces from gusts; $U(t)$ – a function that describes the speed of the gust over time; $\{R_\delta\}$ –

vector representing the work of external forces from the deflection of the control surfaces; $\delta(t)$ – a function that describes the control surfaces deflection over time.

When using non-stationary aerodynamics, the coefficients of the matrices **B** and **D** are no longer constant, but depend on the time and oscillations of the aircraft. Along with the organization of the left parts of the equations, the right parts are formed, corresponding to various physical influences on the aircraft in the air and on the ground, such as gusts of air and deviations of the control surfaces.

The equilibrium equation for an elastic aircraft in horizontal steady-state mode flight can also be obtained based on Equation (1), taking matrices **D** and **H** equal to zero and deriving from other matrices and columns the coefficients responsible for the movement of the aircraft along the longitudinal axis x. When calculating the loads in horizontal flight using a method based on the decomposition of elastic static deformations in a number of forms of natural oscillations. This allows to rationally use some of the results obtained in the calculations of the dynamic load. Aerodynamic forces are determined taking into account the elastic deformations that cause the redistribution of these forces on the bearing surfaces, as well as taking into account the geometric twist of the wing and thrust of the engines. The parameters of turbulence are also important such as the frequency and speed of air gusts because the pattern of turbulence determines the corresponding coefficients of the vector $\{R_U\}$ and are described with the function $U(t)$ (EASA, 2020).

The next step is to solve the integro-differential equations in the time domain using transient non-stationary functions to find the extreme load values. It was also possible to solve these equations in the frequency domain using Fourier transformations from transition functions to determine the frequency characteristics, spectral densities, and maxima of the dynamic response (Wright & Cooper, 2008; Kuznetsov, 2008).

Operational loads are of special interest for the analysis of structural strength. To obtain these operational forces and moments, the calculated increments of dynamic loads during flight in turbulent conditions are summed with loads of horizontal flight.

1.1. Model of turbulence and loads

When determining the impact of continuous turbulence, according to the requirements of Certification Specifications for Large Aeroplanes (CS-25) (EASA, 2020), the atmosphere is considered to be one-dimensional with a gust of speed acting normally (vertically or horizontally) in the direction of the flight of the aircraft (Hoblit, 1988). Random gusts of continuous turbulence are described by Power Spectral Density (PSD) of gusts, proposed by von Karman (Federal Aviation Administration, 2014):

$$\Phi_I(\Omega) = L/\pi \frac{1+8/3\cdot(1.339\cdot L\Omega)^2}{\left[1+(1.339\cdot L\Omega)^2\right]^{11/6}}, \tag{2}$$

where $\Phi_I(\Omega)$ – normalised PSD of atmospheric turbu-

lence, $(m/s)^2/(rad/m)$; Ω – reduced frequency, rad/m; $L = 760\ m$ – scale of turbulence.

The solution for a dynamic reaction from continuous turbulence is fulfilled in the frequency domain (as it is shown in Figure 1), using the RMS values of the reaction. The maximum operational increment of any type of a load to the value of this load in the horizontal flight is determined with the formula (EASA, 2020):

$$P_L = P_{L-1g} \pm U_\sigma \overline{A}, \tag{3}$$

where P_L – limit load; P_{L-1g} – steady 1-g load for the condition; U_σ – limit turbulence intensity in true airspeed; $\overline{A}$ – ratio of RMS incremental load for the condition to RMS turbulence velocity.

As it follows from Equation (3), it is necessary to know the RMS values of increments of the dynamic load increments relative to the loads in the horizontal flight and the actual loads in horizontal flight. There are two methods for obtaining this data. The first is based on the classical spectral analysis in the frequency domain. The second is based on the direct simulation of flights in the time domain to obtain the necessary characteristics of the transients with the subsequent receiving of the RMS values. When solving the system of linear equations, Gauss' method is used to determine the transfer functions of generalized coordinates, and the trapezoidal method or Simpson method is used to calculate the integrals that give the RMS values of loads and correlation coefficients (Kuznetsov, 2008).

1.2. Model of aircraft structure

In both studied methods, the model of the aircraft structure is given with the spatial beam schematization, that means such parts as a wing, a fuselage, etc are modelled with elastic beams that have bending stiffness in two mutually perpendicular plane surfaces and torsion. Each beam is characterized with the distribution of stiffness and mass. To calculate the deformations and loads of such a system, a linear engineering theory of bending and torsion of beams with variable stiffness is used. When schematizing the structure of an aircraft, the wing can be installed relative to the fuselage at the angles of sweep, jamming, and transverse V, and the tailplane can be located either on the fuselage or the fin (T-tail). The beams that simulate the structure of the aircraft, in the general case, can be spaced relative to each other, for example in the case of a high-wing or low-wing aircraft. The connection of the beams with each other can be either absolutely rigid or elastic, characterized by a matrix of coefficients of compliancy for the six degrees of freedom of the joint.

In DTA the main structure of the airplane is modelled with nine elastic beams. Each semi-wing and fuselage are modelled with two beams, so its stiffness axis can be disrupted. All beams, in turn, are evenly divided into several sections (from 2 to 11), which are counted from the junction of the beams to the free end of the suitable construction. Additional cargo and power plants can also be suspended to the wing beams.

The description of the model of an aircraft structure and, accordingly, its finite-element model in IMAD is made using a regular multi-level tree, the nodes of which are sub-structures (Ivanteev et al., 2004). These substructures can be represented as elastic beams. In addition, there is no limit for the number of beams, and arbitrary and uneven division of beams into sections is allowed. But to correctly compare the results of the calculations, a model of the aircraft similar to the model for DTA was constructed.

An important part of the both methods is the calculation of the shapes and frequencies of oscillations of the elastic airplane and suspended objects, which are considered as one system. The shapes and frequencies of the aircraft oscillations (maximum 11 tones) are determined with the help of DTA by solving a common system of integral and linear equations using the method of successive substitution. The peculiarity of the method is that with the presence of suspended objects at each step of the iterative process, the system of equations is additionally solved to determine the forces and moments of the reaction in the mounting nodes. The convergence of the method is controlled both with the frequencies and with the amplitudes of the oscillation forms at a number of selected points. The tones of the aircraft oscillations with the help of IMAD are determined based on partial tones of the substructures using a special algorithm of modal synthesis (Ivanteev et al., 2004; Ivanteev & Steba, 1988). There is no limit in the number of tones in IMAD, but usually, it is enough to take into account 25÷30 tones in the calculations. This may cause some differences in determining the shapes and frequencies of the tones of natural oscillations, so in this study, only the first 9 tones were taken into account.

1.3. Aerodynamic model

Aerodynamic loads are determined by calculating the flow around the aircraft surface. The numerical aerodynamics of the both methods is based mainly on the linear theory. The use of the linear aerodynamics methods makes it possible to divide the main problem of calculating the aerodynamic flows into a set of simple partial problems. These problems include independent changes in the kinematic parameters of the aircraft as a rigid body, as well as the kinematic parameters of elastic deformations and the deviations of aerodynamic control surfaces.

DTA uses the method of circulation (Kuznetsov, 2008) to determine the aerodynamic forces and coefficients, which does not take into account aerodynamic interference between sections. The value of circulation and its distribution on the surface of the aircraft is carried out with the help of the third-party software or based on test results in the wind tunnels.

The main difference of IMAD is the ability to independently calculate the aerodynamic coefficients and forces. Therefore, it is also necessary to describe the geometry of the outer surfaces of an aircraft. Body aerodynamics is set for the fuselage, flat aerodynamics is set for the nacelles, all other units use wing aerodynamics. The same data were used to form the aerodynamic model as well as the geometric model.

To determine aerodynamic coefficients and forces using IMAD, the Doublet-Lattice and Constant Pressure Method (DLM/CPM) was used. In this method, Doublet-Lattice Method (DLM) is used for subsonic modes, for stationary and non-stationary subsonic flows. The aerodynamic surfaces of an aircraft are modelled with panels. The stationary flow uses panels with horseshoe-shaped vortices for wings and panels with pointlike sources for three-dimensional bodies. In the non-stationary flow, oscillating doublets for wings and oscillating pointlike sources for three-dimensional bodies are used (Ivanteev et al., 2004). The panel Method of Constant Pressures (CPM) is used to calculate supersonic modes (Appa, 1987). Unlike DLM for stationary supersonic flows the panels with a constant distribution of vortices at the analysis of lifting surfaces, and the panels with constant sources for bodies are used. For non-stationary aerodynamics, only lifting surfaces are considered in the supersonic flow and only panels with oscillating doublets are used. The threshold flow tangency conditions which were specified in the control points of the panels, reduces the problem to the solution of a system of linear equations.

The numerical solution of this system gives the values of the velocities for the control points of the panels. In addition, when calculating the pressure coefficients on each panel, the axial component of the perturbed velocity and the potential value are used. The aerodynamic coefficients of the aircraft are calculated based on the defined pressure fields using Gauss quadratic formulas. When using discrete vortices, the aerodynamic coefficients are calculated using Zhukovsky's formula (Chuban et al., 2002).

When determining the loads in the horizontal flight, the balancing of the aircraft is performed by deflecting the control surface on the horizontal tail surfaces at an angle determined from the solution of the equilibrium equations of the aircraft.

After obtaining the generalized aerodynamic forces and coefficients for determining the loads, the spectral analysis in the frequency domain is carried out, followed by obtaining the RMS values.

2. Results

The calculations were carried out for the model of a perspective regional turbojet aircraft (RTJ-1X9). To do this, a model of an aircraft structure was designed, the same for both methods. The calculations were carried out for three payload options. The main data of the aircraft models are given in Table 1. The calculated studies were carried out for the flight conditions with cruising mode at a cruise speed V_c, at load conditions following the requirements of certification authorities (EASA, 2020). The visual appearance of the aerodynamic model and the beam-like model of RTJ-1X9, used in IMAD, is demonstrated in Figure 2 and Figure 3.

Table 1. Properties of RTJ-1X9 calculation models (created by Authors)

Aircraft model	E	A	B
Aircraft characteristics			
Aircraft mass G, kg	26270	35270	43700
Fuel mass, kg	1100	1100	9530
Payload, kg	0	9000	9000
Wings area, m^2		87.3	
Wingspan, m		28.9	
Main Aerodynamic Chord (MAC), m		3.40	
Location of the center of gravity, % MAC	0.287	0.332	0.306
Distance from the plane of symmetry of the aircraft to the axis of the engine, m		4.2	
Frequency of the 9th tone of the aircraft's own oscillations			
DTA, Hz	14.04	13.42	12.05
IMAD, Hz	10.43	10.25	10.00
Flight parameters			
Speed of flight, V_c (Equivalent airspeed), m/s		152,76	
Mach number		0.81	
Altitude, m		8930	
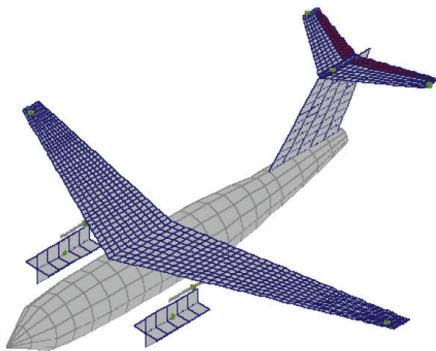
Figure 2. Aerodynamic model of RTJ-1X9 of IMAD (created by Authors)
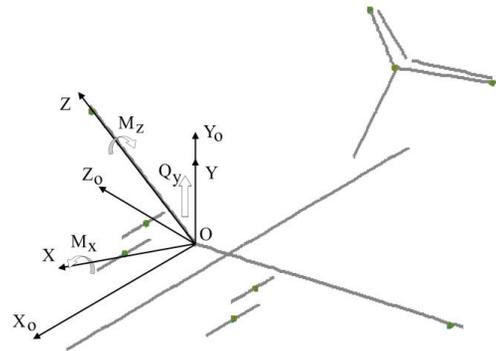
Figure 3. Condensed beam-like model of RTJ-1X9 of IMAD and the loads acting on the wing (created by Authors)

The subject of the analysis of this work is the results of calculations of the loads effecting on the aircraft during the flight in continuous turbulence, which were obtained using the DTA and IMAD methods, such as:

a) the values of the shear force Q_y, and their distribution over the wingspan;

b) the values of the bending moment M_x, and their distribution over the wingspan;

c) the values of the torque M_z, and their distribution over the wingspan;

d) the values of the maximum vertical overload n_y, and their distribution over the wingspan;

e) the values of the maximum vertical $n^e_{y\ MAX}$ and maximum lateral $n^e_{z\ MAX}$ overload in the center of mass of the power plant.

Below, in Figure 4, Figure 5, Figure 6 the change in the maximum calculated values Q_y, M_x, and M_z over the wingspan in the case of dynamic loading during the flight in continuous turbulence for all aircraft models is present-ed. The change in the maximum design overloads over the wingspan in the case of dynamic loading during the flight in continuous turbulence is depicted in Figure 7. Table 2 shows the positive and negative directions of the effect of force factors, which are shown in Figure 4, Figure 5, Figure 6 and Figure 7. Table 3 shows the maximum calculated values of the vertical and lateral overload in the center of the masses of the power plant in the case of dynamic load during the flight in continuous turbulence.

Table 2. The direction of effect of force factors (created by Authors)

Force factor	Designation	"+"	"–"
Shear force	Q_y	force up	force down
Bending moment	M_x	bend up	bend down
Torque	M_z	pitch-up	dive
Vertical overload	n_y	down overload	up overload
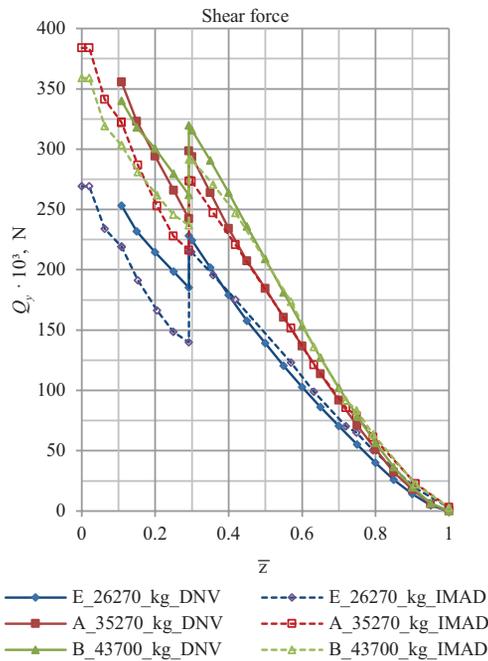
Figure 4. The distribution of the shear force Q_y over the wingspan $\overline{Z}$ depending on the mass of the aircraft (created by Authors)
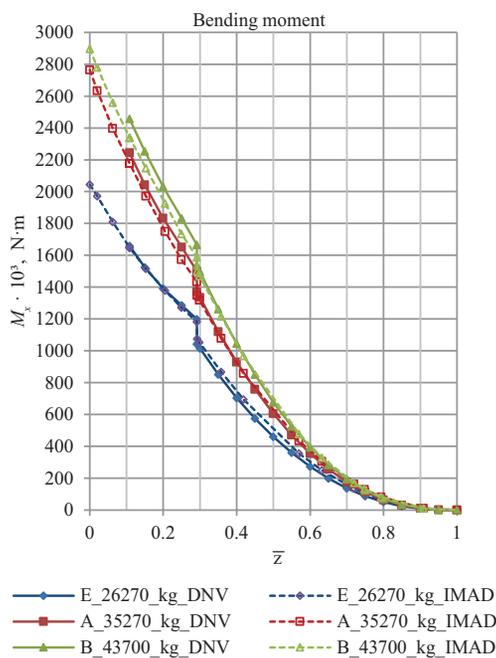
Figure 5. The distribution of the bending moment M_x over the wingspan $\overline{Z}$ depending on the mass of the aircraft (created by Authors)

From Figures 4 and Figure 5, first of all, it can be seen that at higher flight mass of the aircraft, the absolute values of the loads of the shear force Q_y and the bending moment M_x are also greater. However, in Figure 5 it is shown that for the torque M_z at a larger mass of the aircraft, the values of M_z are smaller. The abrupt jump in the load values at the location of the power plant is also well noticeable.

As it can be seen from Figure 4 in the area of the wingspan over $0.4÷0.5$ $\overline{Z}$, IMAD shows higher values of shear force than DTA. However, in root sections, that changes. Figure 5 shows a similar trend. It should be noted that although the mass of the second model of the aircraft (model A, $G = 35270$ kg) is almost in the middle between the other two models (E and B), the values of the loads almost approach to, and sometimes are higher than the values of the shear force of the heavier model B.

Figure 6 demonstrates a significant difference between the results of IMAD and DTA methods. Absolute values of the torque, which are calculated using IMAD, starting from the end of the wing, consistently (excluding the abrupt jump at the location of the power plant) increase over the entire span of the wing console, with a much larger gradient than the torque values, which are calculated using DTA. So, the DTA results rose slightly to the place of installation of the engine, and then after the abrupt jump, practically remain at the same level and even marginally decrease. The values of the abrupt jump for DTA and IMAD differ by a factor of $2÷2.5$.

The maximum values of vertical overloads, as it can be seen in Figure 7, grow significantly on the wingtip, and reach the highest values when studying the model A ($G = 35270$ kg). However, in the root sections of heavier models of an aircraft, the values of overloads are lower. Also, IMAD in the root sections shows lower values, but starting with the range of $0.3÷0.4$ $\overline{Z}$ – higher values than DTA.

As it can be seen in Table 3, at the lowest flight weight of the aircraft, the vertical overload of the power plant is the largest, and at increased aircraft load, it decreases. The value of the lateral overload is higher at the average load weight for DTA and the maximum load weight for IMAD. In general, DTA shows higher values of overload than IMAD.
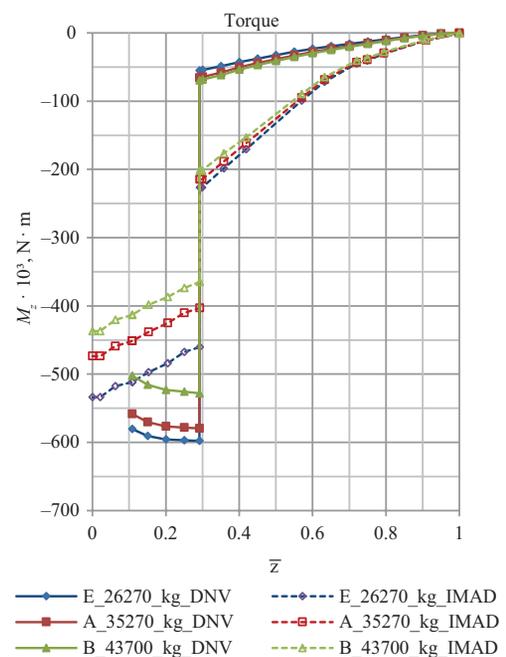
Figure 6. The distribution of the torque M_z over the wingspan $\overline{Z}$ depending on the mass of the aircraft (created by Authors)
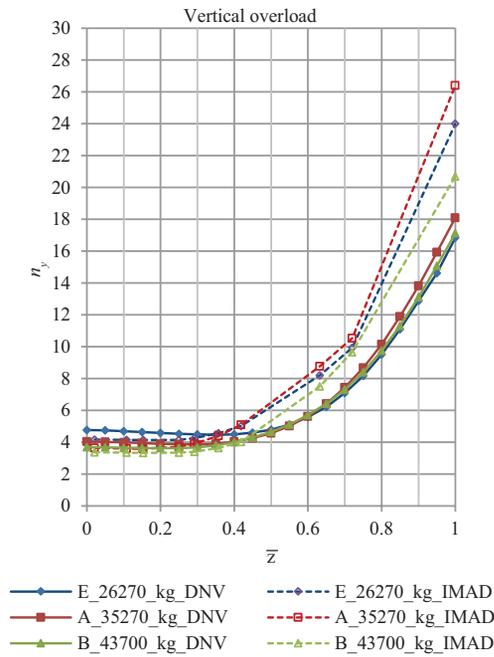
Figure 7. The distribution of the maximum vertical overload n_y over the wingspan $\overline{Z}$ depending on the mass of the aircraft (created by Authors)

Table 3. Maximum calculated values of the vertical and lateral overload in the center of gravity of the power plant depending on the mass of the aircraft (created by Authors)

Model		E	A	B
Mass, kg	Method	26270	35270	43700
$n_{y\ MAX}^{e}$	DTA	6.31	5.14	5.21
	IMAD	4.38	3.81	3.63
$n_{z\ MAX}^{e}$	DTA	2.36	2.89	2.46
	IMAD	2.1	2.4	2.61

3. Discussion

The results of this research show that the values of loads from continuous turbulence calculated using IMAD differ from the values calculated using DTA. The largest difference of the values of the shear force Q_y is observed at an aircraft mass of $G = 26270\ kg$. It is from 16 to 33% on the root part of the wing (from the fuselage to the power plant) when larger values are obtained using the DTA method. At other masses of the aircraft, the difference of values of Q_y does not exceed 10÷16%. Interesting results were obtained when determining the bending moment M_x. The largest difference in values of M_x is now obtained at the maximum mass of the aircraft $G = 43700\ kg$ and is up to 5%. It should be noted that a significant difference in the definition of the values of Q_y and M_x is obtained on the wing end zone $\overline{Z} > 0.75$, it is over 15% and grows to the end of the wing. On the wingtip, larger values of the loads were obtained using the IMAD method. Thus, despite the

significant differences in determining the distribution of the shear force Q_y over the wingspan, very close values of the bending moment M_x are obtained, which is an integral value of the distribution of Q_y over the wingspan.

The significant difference in the values of Q_y and, accordingly of M_x, on the wing end zone is explained by differences in determining the character of the flow around the surface of the aircraft, namely taking into account the air flowing from the upper surface of the wing to the lower, which forms finite inductive vortices. Thus, although the results of the load calculation are quite similar because the mass-inertial characteristics were defined the same for both methods, the significant difference is mainly in the use of different methods for determining aerodynamic loads. The method of circulations used in DTA (Kuznetsov, 2008) does not allow to take into account all the cases of aircraft surface flowing, however, for the specific cases for which the required circulations are calculated, high accuracy of load calculations during the flight in turbulent conditions can be achieved. The panel numerical methods used in IMAD allow high variability of calculation cases, but in this case there is the problem to check the correctness of the aerodynamic coefficients, which are calculated with this method. Since panel methods of aerodynamics, today, are somewhat inferior in accuracy to nonlinear Navier-Stokes Computational Fluid Dynamics (CFD) simulation methods (Voss et al., 2019) or to wind tunnel tests (Boutemedjet et al., 2018; Guimarâes-Neto et al., 2014). However, panel methods, and especially DLM remain the main in solving aeroelastic problems (Mahran et al., 2015; Marqui et al., 2017; Murua et al., 2012).

Unexpected significant differences in the distribution of the torque M_z values over the wingspan (Figure 6) indicate the above-mentioned difference in the prediction of the aerodynamic forces and their distribution on the wing surface using both methods. Thus, at approximately the same values of the shear force Q_y for the corresponding flight masses of the aircraft, there is a difference of 2.5÷4 times in the values of the torque M_z at the wing end zone. These results primarily indicate that the position of the center of pressure in these sections of the wing is different. In the case of using the IMAD method, the calculated center of pressure in the respective sections of this part of the wing is located further from the axis of rigidity of the wing than in the case of specified circulations in the DTA method. A similar situation is observed with the location of the center of pressure on the root part of the wing, but it is also necessary to take into account the impact of the power plant, which creates an abrupt jump in the torque M_z values at the location of the engine. In the root part of the wing, the character of the change in the distribution of the values of the torque M_z differs from the character of the distribution on the wing end zone. In the case of IMAD, the torque M_z increases over the wingspan almost linearly. And in the case of DTA, the value of the torque M_z almost does not change, and even decreases slightly. This indicates a different consideration

of the interference between the wing and the fuselage sing both methods. Since the DTA method uses data on the features of the flowing of the surface of the aircraft obtained by other methods, such as wind tunnel tests and numerical panel method (Bondar, 2014), these data can be considered more accurate.

The previously mentioned abrupt jump of the values of loads at the location of the engine, in Figure 4 and Figure 6 is different, both for different aircraft weights and for the selected methods of load calculations. Although the mass of the power plant is the same for all the cases. This is because the engine is additionally affected by the vertical overload. The maximum value of the vertical overload in the center of gravity of the power plant is higher in DTA, by about 35÷44% relative to IMAD, but in the Equation (3) to calculate the operating load the RMS of the increase in the dynamic load is used, which also strongly depends on the shape of the aircraft's own oscillations. Since only the first 9 tones were taken into account in the calculations, this could cause some differences in the results of the calculations. This effect needs further study. In Figure 5, the abrupt jump is almost the same, because in this case it is determined by the torque on the jet engine turbine shaft.

Also, it should be noted that in the location of the center wing box, at an aircraft mass of 35,270 kg, the values of the shear force Q_y are superior to the values at a mass of 43,700 kg (Figure 4). This can be explained in this way: the main difference between these two models is that the additional mass of fuel is placed in the wing consoles and has little effect on the upper-fuselage part of the wing. At a lower mass of the aircraft this all leads to greater overload in the center of gravity of the aircraft and partially in the root of the wing, as shown in Figure 6, and accordingly at the same mass of this part of the aircraft leads to greater values of the dynamic load.

Conclusions

In this study, two methods were compared (DTA and IMAD) aimed at the determination of the external loads on the aircraft structure from the effects of dynamic response. The comparison was made through calculations of the loads acting on the elastic wing of a turbojet aircraft during flight in conditions of continuous atmospheric turbulence. To do this, the model of an aircraft design was created, the same for both methods. The calculation conditions were also defined the same for both methods. The obtained results were also compared for three payload options at cruising flight modes.

From the outcome of our investigation it is possible to conclude that, in general, the values of the loads calculated using IMAD are lower than the values calculated using DTA. Except for the torque values on the end parts of the wing. The main differences in the results are caused by the use of different methods of describing the aerodynamic surfaces of the aircraft and the methods of determining the aerodynamic loads. Thus, the use of IMAD allows to reduce the requirements for the structure strength of the aircraft wing, which will lead to a decrease in the mass of the wing, but then will also increase the risk of the structural failure during testing or in flight. In addition, IMAD allows to create more complex designs of an aircraft and to calculate independently the aerodynamic forces effecting the surface of the aircraft. The ability to independently calculate the aerodynamic forces makes it more attractive to use the IMAD method in cases when it is necessary to analyze a significant number of calculated cases. The use of the DTA method is more attractive, from the point of view of ensuring the safety and strength of the aircraft structure and for the cases when the exact values of the distribution of aerodynamic forces on the aircraft surface are known what is the so-called circulation. Thus, it is possible to make the following recommendation: to calculate the loads during the flight in turbulent conditions using IMAD. Then the loads obtained in the critical points of the calculated flight area can be confirmed using the DTA method. The envelopes of external loads obtained using both methods can continue to be used to design the aircraft structure.

This work focuses on the wings of a turbojet aircraft, however, the methods described here can also be applied to other types of aircraft with high aspect ratio wing, or to determine the load effecting on the fuselage and the tail unit of the aircraft.

In future studies should be taken into account not only the standard requirements but also the nonuniform distribution along a wingspan for discrete gusts and continuous turbulence. In addition, in further calculations, the influence of the remote control system and the impact of the gust load alleviation system must be considered. This requires some refinement of the methods which have been studied in this paper. Also, in the future, it is possible to compare the methods of DTA and IMAD studied in this article with the methods used in the NASTRAN solution 146 and with flight test data.

Author contributions

YuB conceived the study and was responsible for the development of the data analysis. BH was responsible for the development of the mathematical model of the aircraft, loads calculation, and data analysis, he also wrote the article and was responsible for the submission process.

Disclosure statement

Authors declare that they do not have any competing financial, professional, or personal interests from other parties.

References

Appa, K. (1987). Constant pressure panel method for supersonic unsteady airload analysis. *Journal of Aircraft*, *24*(10), 696–702. https://doi.org/10.2514/3.45509

Bondar, Y. I. (2014). Metod privedenija raschjotnyh ajerodinamicheskih harakteristik k rezul"tatam drenazhnyh ispytanij modeli samoljota transportnoj kategorii [Method of reducing design aerodynamic characteristics to the results of drain tests of a transport category aircraft model]. *Vestnik of the Samara State Aerospace University, 1*(43), 22–29. https://doi.org/10.18287/1998-6629-2014-0-1(43)-22-29

Boutemedjet, A., Samardžić, M., Rebhi, L., Rajić, Z., & Mouadaet, T. (2018). UAV aerodynamic design involving genetic algorithm and artificial neural network for wing preliminary computation. *Aerospace Science and Technology*, *84*, 464–483. https://doi.org/10.1016/j.ast.2018.09.043

Chuban, V. D., Ivanteyev, V. I., Chudayev, B. J., Avdeyev, E. P., & Shvilkin, V. A. (2002). Numerical simulation of flutter validated by flight-test data for TU-204 aircraft. *Computers and Structures*, *80*(32), 2551–2563. https://doi.org/10.1016/S0045-7949(02)00221-3

European Union Aviation Safety Agency. (2020). *Certification specifications and acceptable means of compliance for large Aeroplanes CS-25. Amendment 26.* https://www.easa.europa.eu/sites/default/files/dfu/cs-25_amendment_26_0.pdf

Federal Aviation Administration. (2014). *Advisory Circular 25.341-1 – dynamic gust loads.* https://www.faa.gov/documentLibrary/media/Advisory_Circular/AC_25_341-1.pdf

Fomichev, P. A., Lavro, N. A., & Vakulenko, S. V. (2014). Sootnoshenie mezhdu integral"nymi povtoryaemostyami amplitud i maksimumov peregruzki pri polete v turbulentnoi atmosphere [Relationship between cumulative probabilities of equivalent amplitudes and maximums of load factors during the flight in turbulent atmosphere]. *Civil Aviation High Technologies*, *199*, 101–107.

Giesseler, H.-G., Kopf, M., Varutti, P., Faulwasser, T., & Findeisen, R. (2012). Model predictive control for gust load alleviation. *IFAC Proceedings, 45*(17), 27–32. https://doi.org/10.3182/20120823-5-NL-3013.00049

Guimarâes-Neto, A. B., da Silva, R. G. A., & Paglione, P. (2014). Control-point-placement method for the aerodynamic correction of the vortex- and the doublet-lattice methods. *Aerospace Science and Technology*, *37*, 117–129. https://doi.org/10.1016/j.ast.2014.05.007

Hevko, B. A., & Bondar, Yu. I. (2019, December). An algorithm for determining loads when flying in disquiet air. In *Materialy naukovo-praktychnoi' konferencii' studentiv ta molodyh vchenyh* [Materials of scientific and practical conference of students and young scientists], *Avia-raketobuduvannja: perspektyvy ta naprjamky rozvytku* [Aircraft rocket science: prospects and directions of development] (p. 7). Kyiv, Ukraine. https://arb.kpi.ua/uk/science/conferences/naukovo-praktychna-konferentsiia-avia-raketobuduvannya-perspektyvy-ta-napryamky-rozvytku

Hoblit, F. M. (1988). *Gust loads on aircraft: Concepts and applications.* AIAA Education series. Aerospace Research Central. https://doi.org/10.2514/4.861888

Ivanteev, V. I., Snisarenko, T. V., & Chuban, V. D. (2004). *Interaktivnoe mnogodisciplinnoe proektirovanie letatelnyh apparatov. Versija 10.6* [Interactive multi-disciplinary aircraft design. Ver.10.6]. TsAGI.

Ivanteev, V. I., & Steba, M. A. (1988). Metody rascheta sobstvennyh form i chastot kolebanij samoleta na osnove integral"nyh uravnenij dvizhenija [Methods for calculating the natural forms and frequencies of aircraft oscillations based on integral equations of motion]. *Trudy TsAGI, 2405*, 22–35.

Karpel, M., Moulin, B., & Chen, P. C. (2005). Dynamic response of aeroservoelastic systems to Gust excitation. *Journal of Aircraft*, *42*(5), 1264–1272. https://doi.org/10.2514/1.6678

Kim, T.-U., & Hwang, I. H. (2004). Reliability analysis of composite wing subjected to gust loads. *Composite Structures, 66*(1–4), 527–531. https://doi.org/10.1016/j.compstruct.2004.04.072

Kuznetsov, O. A. (2008). *Dinamicheskie nagruzki na samolet* [Dynamic aircraft loads]. Fizmatlit.

Lone, M., & Dussart, G. (2019). Impact of spanwise non-uniform discrete gusts on civil aircraft loads. *The Aeronautical Journal, 123*(1259), 93–120. https://doi.org/10.1017/aer.2018.148

Mahran, M., Hani Negm, H., & Adel El-Sabbagh, A. (2015). Aero-elastic characteristics of tapered plate wings. *Finite Elements in Analysis and Design*, *94*, 24–32. https://doi.org/10.1016/j.finel.2014.09.009

Marqui, C. R., Bueno, D. D., Goes, L. C. S., & Gonçalves, P. J. P. (2017). A reduced order state space model for aeroelastic analysis in time domain. *Journal of Fluids and Structures*, *69*, 428–440. https://doi.org/10.1016/j.jfluidstructs.2017.01.010

Murua, J., Palacios, R., & Graham, J. M. R. (2012). Applications of the unsteady vortex-lattice method in aircraft aeroelasticity and flight dynamics. *Progress in Aerospace Sciences*, *55*, 46–72. https://doi.org/10.1016/j.paerosci.2012.06.001

Reytier, T., Bes, C., Marechal, P., Bianciardi, M., & Santgerma, A. (2012). Generation of correlated stress time histories from continuous turbulence Power Spectral Density for fatigue analysis of aircraft structures. *International Journal of Fatigue, 42*, 147–152. https://doi.org/10.1016/j.ijfatigue.2011.08.013

Rodden, W. P., & Johnson, E. H. (1994). *MSC/NASTRAN Aeroelastic Analysis User's Guide.* The MacNeal-Schwendler Corp. Los Angeles.

Rodden, W. P., Taylor, P. F., & McIntosh, S. C. (1998). Further refinement of the subsonic doublet-lattice method. *Journal of Aircraft*, *35*(5), 720–727. https://doi.org/10.2514/2.2382

Rodden, W. P., Taylor, P. F., McIntosh, S. C., & Baker, M. L. (1999). Further convergence studies of the enhanced doublet-lattice method. *Journal of Aircraft, 36*(4), 682–688. https://doi.org/10.2514/2.2511

Tang, B., Wu, Z., & Yang, C. (2016). Aeroelastic scaling laws for gust load alleviation control system. *Chinese Journal of Aeronautics, 29*(1), 76–90. https://doi.org/10.1016/j.cja.2015.12.001

Voss, G., Schaefer, D., & Vidy, C. (2019). Investigation on flutter stability of the DLR-F19/SACCON configuration. *Aerospace Science and Technology*, *93*, 105320. https://doi.org/10.1016/j.ast.2019.105320

Wright, J. R., & Cooper, J. E. (2008). *Introduction to aircraft aeroelasticity and loads.* John Wiley & Sons. https://doi.org/10.2514/4.479359

Yang, Y., Yang, Ch., & Wu, Zh. (2019). Aeroelastic dynamic response of elastic aircraft with consideration of two-dimensional discrete gust excitation. *Chinese Journal of Aeronautics, 33*(4), 1228–1241. https://doi.org/10.1016/j.cja.2019.09.008

ZONA Technology. (2017). *ZAERO Version 9.3 Theoretical Manual.* ZONA Technology, Inc., ZONA 01-17.0, Scottsdale, AZ. https://www.zonatech.com/Documentation/ZAERO%209.3_THEO_Full_Electronic.pdf